CRC-AIDED ITERATIVE OPTIMAL DETECTION FOR MIMO-OFDM SYSTEMS WITH LINEAR PRECODING

Felip Riera-Palou and Guillem Femenias

Mobile Communications Group (Dept. of Mathematics and Informatics), University of the Balearic Islands
Crta. Valldemossa km 7.5, 07122, Mallorca (Illes Balears), Spain
phone: + (34) 971-173196, fax: + (34) 971-173003, email: {felip.riera,guillem.femenias}@uib.es

ABSTRACT

This paper proposes a novel receiver structure based on soft information for linearly precoded MIMO-OFDM systems. The architecture combines an MMSE-based front end with an iterative technique based on maximum likelihood detection (MLD) in a structure that exhibits two very attractive features. Firstly, it can fully exploit the diversity benefits of spreading the information symbols in the space and frequency domains by optimally estimating them. Secondly, and under the realistic assumption of the presence of a cyclic redundancy check (CRC) mechanism, the far more computationally demanding MLD component needs only be used when the MMSE front end has failed. Simulation results reveal that the MLD iterative mechanism adds only a negligible amount of computations to the simple MMSE detector while significantly improving its performance.

1. INTRODUCTION

Most state-of-the-art wireless systems are based on a multicarrier multiantenna physical layer that combines multiple antennae at transmission/reception (MIMO) and orthogonal frequency division multiplexing (OFDM) resulting in the so-called MIMO-OFDM architecture. Methods that exploit channel state information at the transmitter (CSIT) have been intensively investigated in recent times. Nevertheles, the optimal strategy from an information theoretic point of view to exploit this knowledge has been known for nearly three decades in the form of a scheme known as dirty paper coding (DPC) [1]. The idea behind DPC is to exhaustively search for the best interference pre-cancelling pattern, however, its high computational cost motivates the need for simpler alternatives. A fundamental contribution in this direction was presented in [2], where a framework based on convex optimisation was introduced to optimally design the system with respect to different objective functions and constraints with the additional restriction that only linear processing was allowed at transmission and reception. The proposed scheme defines transmit and receiver filters that are based on the singular value decomposition (SVD) of the whitened channel matrix and performs a distribution of the available power among the different transmit modes using waterfilling. It is further stated that subcarrier cooperation strategies are inherently superior to subcarrier non-cooperative counterparts due to its stronger robustness against fading. Subcarrier cooperation is typically implemented in practice by spreading the information in the spatial and frequency domains using unitary rotation matrices, a technique well-known to lead to significant diversity gains in the context of multicarrier systems [3]. In [4] precoding strategies combined with forward error correction were considered, again in the context of linear detectors. The linear processing framework has the low computational complexity as one of its major highlights, however, it opens the door to question what extra benefits can be attained when the receiver has enough resources that enable the use of more sophisticated strategies. To this end, [5] has recently explored the possibility of using a non-linear detector, namely, maximum likelihood detection (MLD), to estimate the linearly precoded symbols. It was shown that MLD leads to significant advantages in terms of error rate over linear detection whenever information symbols are spread onto more than one transmission mode (in either frequency or space) as in this case, unlike non-spread setups, the overall transmission chain made of precoder, channel and receive filter is not diagonal. The main drawback of MLD is its large computational complexity as even smart implementations (i.e., sphere decoding) are computationally demanding at low SNRs, where practical systems usually operate [6].

This paper introduces a near-optimal low complexity detection strategy based on soft information in the context of bit interleaved coded modulation (BICM) systems. Exploiting the availability of a CRC on each frame that allows the receiver to determine whether a frame has been successfully received or not, an iterative procedure is introduced that combines linear and non-linear processing in such a way that optimal performance is achieved with a much lower complexity than that of a pure MLD receiver.

2. SYSTEM MODEL

2.1 General transmitter architecture

This work is concerned with a BICM-MIMO-OFDM system similar to the architectures described in modern wireless standards such as IEEE 802.11n. Transmitter

Acknowledgments: this work is supported in part by MEC and FEDER under project COSMOS (TEC2008-02422), Spain.

Notation: vectors and matrices are denoted by bold lower case and bold upper case letters, respectively. Superscripts ^{T} and ^{H} denote transpose and complex transpose (Hermitian), respectively. The operator $\otimes$ represents the Kronecker product of two matrices. $\boldsymbol{I}_k$ denotes the k-dimensional identity matrix and $\mathcal{D}(\boldsymbol{x})$ is used to represent a (block) diagonal matrix having $\boldsymbol{x}$ at its main (block) diagonal and $[\boldsymbol{A}]_{i,j}$ indicates the (i,j)-element of matrix $\boldsymbol{A}$. Finally, $(\cdot)^+ = \max\{0, \cdot\}$.

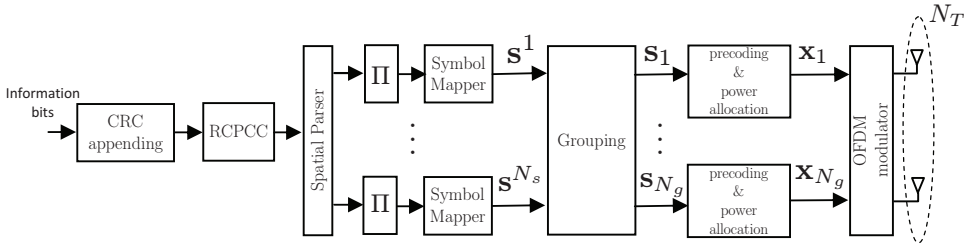

Figure 1: Transmitter block diagram for CRC-aided linearly precoded system.

(Tx) and receiver (Rx) are equipped with N_T and N_R antennae, respectively, which are used to simultaneously transmit N_s ($N_s \leq N_T$) data streams. The available system bandwidth is exploited by means of N_c subcarriers out of which N_d are used to carry data and N_p are destined to control information (pilot signals and guard bands). Perfect CSI is available at Tx and Rx.

Incoming information bits are first segmented into frames and, as shown in Fig. 1, each frame has a CRC checksum appended. Subsequently, every frame is encoded using an R_c-rate compatible punctured convolutional coder (RCPCC) and the resulting coded bits are distributed among N_s streams corresponding to different spatial branches. On each spatial branch, bits are interleaved and mapped onto modulation symbols from an M-ary modulation alphabet resulting in the symbol streams $\left\{\mathbf{s}^1, \cdots, \mathbf{s}^{N_s}\right\}$.

Note that the combination of spatial parsing and (per-stream) interleaving results in a space-frequency interleaving of the coded bits. Each spatial stream is then organized into segments of N_d symbols eventually becoming OFDM symbols (with the addition of N_p pilot/null subcarriers). Furthermore, every segment is partitioned into N_g groups of $Q = N_d/N_g$ symbols each that will be used to implement the subcarrier cooperation by means of group-orthogonal code-division multiplexing [3] (i.e., frequency spreading). A set of Q subcarriers, each with N_s spatial modes, that serve to transmit $N_s \times Q$ symbols denoted by $\mathbf{s}_g = \left[(\mathbf{s}_g^1)^T \cdots (\mathbf{s}_g^{N_s})^T\right]^T$, with $1 \leq g \leq N_g$, will be referred here as a group. Due to subcarrier orthogonality, and for a given channel realisation, groups are independent from each other and therefore, further processing can focus on an arbitrary single group formed by the symbols $\mathbf{s}_g$. The mapping from information to transmit symbols is done by

$$\mathbf{x}_g = \mathbf{W}_g \mathbf{s}_g, \tag{1}$$

where $\mathbf{W}_g$, with dimensions $N_T Q \times N_s Q$, represents the precoding matrix that takes care of matching the transmitted signal to the channel conditions, spreading the information symbols in the space and/or frequency domains and also performing the power allocation. The resulting precoded symbols are then supplied to an OFDM modulator typically consisting of an IFFT plus the addition of a cyclic prefix (CP).

The channel between an arbitrary pair of Tx and Rx antennas is assumed to be frequency-selective with an scenario-dependent power delay profile common to all Tx-Rx pairs and whose individual tap variations follow a Rayleigh distribution. The channel is assumed to remain static over the duration of a frame and vary independently from frame to frame (block Rayleigh fading). The frequency response of the channel linking Tx-antenna i and Rx-antenna j, evaluated over the Q subcarriers assigned to group g over an arbitrary frame, is denoted by $\mathbf{h}_g^{i,j} = [h_{g,1}^{i,j} \ldots h_{g,Q}^{ij}]^T$. Considering the spatial correlation introduced by the transmit and receive antenna arrays, the spatially correlated channel frequency response on subcarrier q of group g can be expressed as

$$\mathbf{H}_{g,q} = \mathbf{R}_{RX}^{1/2} \tilde{\mathbf{H}}_{g,q} \left(\mathbf{R}_{TX}^{1/2}\right)^T, \tag{2}$$

where $\mathbf{R}_{RX}$ and $\mathbf{R}_{TX}$ are $N_R \times N_R$ and $N_T \times N_T$ matrices denoting the receive and transmit correlation, respectively, and $\tilde{\mathbf{H}}_{g,q}$ is an $N_R \times N_T$ matrix made of iid random variables defined as $\tilde{\mathbf{H}}_{g,q} = \left[h_{g,q}^{i,j}\right]_{i=1,j=1}^{N_R,N_T}$.

2.2 Precoding

Under the assumption of availability of CSIT, the channel information can be utilised when designing the precoder $\mathbf{W}_g$. It is shown in [2] that a practical (uncoded/hard decoded) BER minimisation approach consists of employing transmit/receiver filters targeting the minimisation of the mean-square error (MSE) in combination with a rotation matrix at Tx to ensure that performance is not dominated by the worst transmission mode. Moreover, subcarrier cooperation is shown to be more robust against fading than non-cooperative alternatives. In theory all subcarriers would need to be jointly treated in order to minimise the objective error function. However, in practice, it is well known that joint processing of just a few subcarriers is enough for most practical purposes [3]. Taking into account the group-based operation of our system, the optimum transmit filter is defined by

$$\mathbf{W}_g = \mathcal{D}\left(\mathbf{U}_{g,1}, \cdots, \mathbf{U}_{g,Q}\right) \mathbf{\Sigma}_g \mathbf{C}, \tag{3}$$

where $\mathbf{C}$ is an $N_s Q \times N_s Q$ unitary matrix, $\mathbf{U}_{g,q}$ has as columns the eigenvectors of $\mathbf{R}_{g,q} = (1/\sigma^2)\mathbf{H}_{g,q}^H \mathbf{H}_{g,q}$ corresponding to its $N_s Q$ largest eigenvalues and $\mathbf{\Sigma}_g = \mathcal{D}(\sigma_{g,1} \cdots \sigma_{g,N_s Q})$ is an $N_s Q \times N_s Q$ matrix performing the power allocation on the selected transmission modes with the zero entries causing to leave unused modes (i.e. $N_s < N_T$) with no power allocated to them. The power loading coefficients are computed through MSE-

waterfilling [2],

$$\sigma_{g,m} = \sqrt{\left(\mu^{-1/2}\lambda_{g,m}^{-1/2} - \lambda_{g,m}^{-1}\right)^{+}}, \quad (4)$$

with $1 \leq m \leq N_s Q$, where $\mu^{-1/2}$ represents the water-level constant to limit the transmission power level and $\lambda_{g,m}$ denotes the mth largest eigenvalue of $\mathcal{D}([\mathbf{R}_{g,1} \cdots \mathbf{R}_{g,Q}])$. Note that the power allocation defined by (3) operates at group level. This implies that in configurations where $N_s < N_T$ it is possible that subcarriers forming a group are unevenly loaded.

The spreading matrix $\mathbf{C}$ is a unitary transform that spreads the incoming symbol in the frequency and space dimension, which is in general given by,

$$\mathbf{C} = \left(\mathbf{I}_{N_s/R} \otimes \mathbf{C}_{spa}\right) \otimes \mathbf{C}_{fre}, \quad (5)$$

where $\mathbf{C}_{spa}$ is the spatial spreading matrix with R denoting the number of spatial modes over which information is spread, and $\mathbf{C}_{fre}$ is a $Q \times Q$ matrix representing the frequency spreading (e.g., the degree of subcarrier cooperation). Typical choices for $\mathbf{C}_{spa}$ and $\mathbf{C}_{fre}$ are Hadamard or Fourier matrices. For notational simplicity, and without loss of generality, it is assumed from this point onwards that $R = N_s$ so that $\mathbf{C} = \mathbf{C}_{spa} \otimes \mathbf{C}_{fre}$. Note that the form of $\mathbf{C}$ has very important consequences from both, the performance and the complexity points of view. On one hand, choosing $\mathbf{C} = \mathbf{I}_{N_s Q}$ implies no information spreading, hence, as pointed out in [2], the overall transmit-channel-receive system is fully diagonalized and optimal detection is simple to implement although this comes at the cost of a potential diversity loss. On the other hand, any choice of $\mathbf{C} \neq \mathbf{I}_{N_s Q}$ results in information spreading and a potential diversity gain although, in this case, linear processing at the receiver side is not optimal anymore.

3. CRC-AIDED RECEIVER

3.1 Reception equation

The receiving procedure, depicted on Fig. 2, begins with the cyclic prefix removal (CPR) and FFT processing step to recover the baseband samples. The posterior subcarrier selection serves to emphasize that subsequent processing is performed on a group basis and effectively means that subcarriers belonging to the same group are jointly processed while the different groups can be potentially processed in parallel. Assuming the CP exceeds the duration of the channel thus avoiding any interblock interference (IBI), the received samples for group g for an arbitrary OFDM symbol/frame can be expressed as[1]

$$\mathbf{r}_g = \mathbf{H}_g \mathbf{W}_g \mathbf{s}_g + \mathbf{n}_g, \quad (6)$$

where $\mathbf{H}_g = \mathcal{D}([\mathbf{H}_{g,1} \cdots \mathbf{H}_{g,Q}])$ is the frequency-domain channel matrix for group g. The $N_R Q \times 1$ vector $\mathbf{n}_g$ corresponds to the noise samples affecting group g whose entries are assumed to be i.i.d. and drawn from a zero-mean Gaussian distribution with variance σ^2. It is assumed that, on average, each subcarrier has unit energy available to transmit N_s symbols and that the channel frequency response is normalised so that the signal-to-noise ratio per subcarrier can be defined as $E_s/N_0 = 1/(N_s\sigma^2)$.

[1]Successive OFDM symbols are independent from each other, thus allowing all time-related indexes to be dropped.

3.2 Iterative soft detector

As shown in Fig. 2, the received baseband samples, $\{\mathbf{r}_1, \cdots, \mathbf{r}_{N_g}\}$ are supplied to a soft MMSE detector who is in charge of estimating the soft information in the form of log-likelihood ratios (LLR) of the transmitted symbols. The MMSE receive filter is defined as a function of the precoding and channel matrices as

$$\mathbf{G}_g = \left(\mathbf{H}_g \mathbf{W}_g \mathbf{W}_g^H \mathbf{H}_g^H + \sigma^2 \mathbf{I}_{N_R Q}\right)^{-1} \mathbf{H}_g \mathbf{W}_g. \quad (7)$$

In order to derive soft estimates, the post-MMSE receive filter SNR for an arbitrary group symbol j, with $1 \leq j \leq N_s Q$, is first derived as

$$SNR_j = \frac{1}{\left[\left(\frac{1}{\sigma^2}\mathbf{W}_g^H \mathbf{H}_g^H \mathbf{H}_g \mathbf{W}_g + \mathbf{I}_{N_s Q}\right)^{-1}\right]_{j,j}} - 1. \quad (8)$$

Based on [7], the LLR for the in-phase bit on the pth position of the transmitted symbol j, is given by

$$\mathcal{L}^{MMSE}(s_j, b_{I,p}) = \frac{SNR_j}{4} D_{I,p}, \quad (9)$$

where $D_{I,p}$ is given by the mappings defined in [7, (14)-(18)]. LLRs for the bits in quadrature are computed using an analogous procedure. The resulting LLR values, $\boldsymbol{\mathcal{L}}^{MMSE}$ in Fig. 2, are subsequently de-mapped, deinterleaved and de-parsed to form the coded bit stream that is finally supplied to a Viterbi decoder to yield the estimated information bits. Finally, the CRC check is performed to determine whether the frame has been correctly received or not. In the former case the soft-decoded information can already be passed to the higher protocol layers while in the latter case, iterative processing begins by feeding back the extrinsic information.

It is worth stressing that if $\mathbf{C} = \mathbf{I}_{N_s Q}$, the channel is diagonalized by the transmit and receive filters (i.e.,$\mathbf{G}_g \mathbf{H}_g \mathbf{W}_g$ is a diagonal matrix) thus fully decoupling the transmitted symbols in space and frequency. For any other choice of $\mathbf{C}$, the overall system chain is not diagonal anymore and this fact has two important consequences. First, the non-diagonal structure makes MMSE-based reception suboptimal and opens the door to the use of more powerful alternatives such as ML (optimal) detection. Secondly, whereas in conjunction with MMSE, iterative decoding does not bring along any significant performance benefit [8] (as predicted by the almost flat EXIT characteristic curve), when the turbo principle is applied to an MLD-based receiver, it significantly improves the performance with respect to non-iterated schemes. Consequently, the detection strategy is changed from MMSE to ML detection implemented by means of the list sphere detector (LSD) [9], an efficient method to conduct an exhaustive search among a set of candidates (i.e. ML detection) that results in the most likely estimate alongside a list with the closest candidates. This list can then be used to compute the LLR for each bit. To this end the transformation $\mathbf{s}_g = \mathcal{M}(\mathbf{b})$ is defined as the modulation mapping

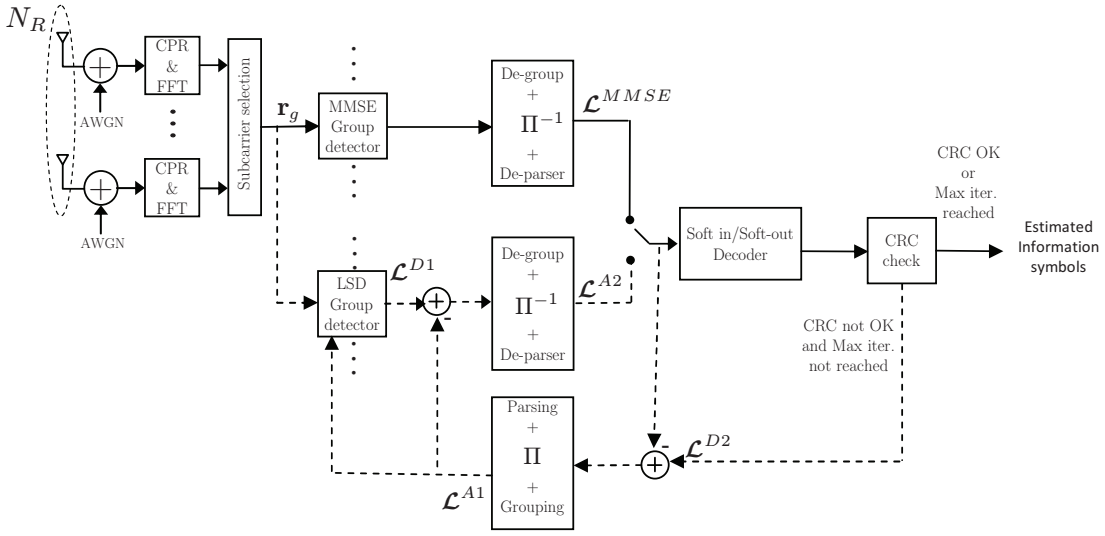

Figure 2: Receiver block diagram for CRC-aided linearly precoded system based on iterative hybrid linear/non-linear detection. Direct path processing is shown with solid arrows and iterative path processing with dashed arrows.

to arrive to symbol vector $\mathbf{s}_g$ from the corresponding group bits $\mathbf{b} = \begin{pmatrix} b_1 & b_2 & \dots & b_{N_b} \end{pmatrix}^T$ (to simplify notation, the group index is skipped when referring to the bits) where $N_b = N_s Q \log_2 M$. Making use of the max-log approximation, the LLR for a given bit, b_p (belonging to an arbitrary group g) can be approximated by [9]

$$\mathcal{L}^{D1}(b_p) \approx \frac{1}{2} \max_{\mathbf{b} \in \mathcal{B}_{p,+1}} \left\{ -\frac{1}{\sigma_n^2} \|\mathbf{r}_g - \mathbf{A}_g \mathcal{M}(\mathbf{b})\|^2 + \mathbf{b}_{[p]}^T (\boldsymbol{\mathcal{L}}^{A1})_{[p]} \right\} - \frac{1}{2} \max_{\mathbf{b} \in \mathcal{B}_{p,-1}} \left\{ -\frac{1}{\sigma_n^2} \|\mathbf{r}_g - \mathbf{A}_g \mathcal{M}(\mathbf{b})\|^2 + \mathbf{b}_{[p]}^T (\boldsymbol{\mathcal{L}}^{A1})_{[p]} \right\}, \quad (10)$$

where $\mathbf{A}_g = \mathbf{H}_g \mathbf{W}_g$ and the characters $\mathcal{B}_{p,+1}$ and $\mathcal{B}_{p,-1}$ represent the sets of 2^{N_b-1} bit vectors whose p^{th} position is a '+1' or '-1', respectively. The $(N_b-1)\times 1$ vector $(\boldsymbol{\mathcal{L}}^{A1})_{[p]}$ contains the a-priori LLR for each bit in $\mathbf{b}$ except for the p^{th} bit. Note that $\boldsymbol{\mathcal{L}}^{A1}$ is obtained by parsing, interleaving and grouping the most recent extrinsic information given by

$$\boldsymbol{\mathcal{L}}^{A1} = \begin{cases} \boldsymbol{\mathcal{L}}^{D2} - \boldsymbol{\mathcal{L}}^{MMSE}, & \text{for the first iteration} \\ \boldsymbol{\mathcal{L}}^{D2} - \boldsymbol{\mathcal{L}}^{A2}, & \text{otherwise,} \end{cases}$$

where $\boldsymbol{\mathcal{L}}^{D2}$ represents the output LLRs of the decoder.

Moderate values of M and/or Q make the sets $\mathcal{B}_{p,+1}$ and $\mathcal{B}_{p,-1}$ extremely large, making the search in (10) computationally unfeasible. To address this issue, LSD limits the search to the sets $\hat{\mathcal{B}}_{p,+1} = \mathcal{B}_{p,+1} \cap \mathcal{C}$ and $\hat{\mathcal{B}}_{p,-1} = \mathcal{B}_{p,-1} \cap \mathcal{C}$ where $\mathcal{C}$ is the set containing the bit vectors corresponding to the N_{cand} group candidates closer, in an Euclidean sense, to the received group vector, i.e., $\mathcal{C} = \left\{ \mathbf{b}^1, \dots, \mathbf{b}^{N_{cand}} \right\}$ where $\mathbf{b}^j = \mathcal{M}^{-1}(\tilde{\mathbf{s}}_g^{[j]})$ with $\left\{ \tilde{\mathbf{s}}_g^{[1]}, \dots, \tilde{\mathbf{s}}_g^{[N_{cand}]} \right\}$ being the N_{cand} group candidates for which $\|\mathbf{r}_g - \mathbf{A}_g \mathbf{s}_g\|^2$ is smallest [9].

When iterating, each group detector has as inputs both, the received samples $\mathbf{r}_g$ and the a-priori LLRs for the bits in the group ($\boldsymbol{\mathcal{L}}^{A1}$), which are then combined by the LSD to yield the a-posteriori LLRs for each group ($\boldsymbol{\mathcal{L}}^{D1}$). As typically done in iterative schemes, only new (i.e., extrinsic) information is interchanged among the different subsystems. To this end, the decoder output is subtracted from its input to derive the extrinsic information, which is fed back to the detection stage.

The iterative procedure terminates whenever the CRC test indicates that the frame has been successfully decoded or a maximum number of iterations has been reached, in which case is up to the system designer to decide what strategy should be followed.

4. NUMERICAL RESULTS

Simulations have been conducted in a software testbed conforming to the recent IEEE 802.11n specifications. The system is configured with $N_T = N_R = N_s = 2$ (i.e., fully loaded system) and operating on $N_c = 64$ subcarriers ($N_d = 52$, $N_p = 12$). The transmitter uses a $1/2-$rate convolutional channel coder with generator polynomials [133 171]. Perfect CSI is assumed at both ends of the communication link. The correlation coefficient between collocated antenna elements that define matrices $\mathbf{R}_{TX}$ and $\mathbf{R}_{RX}$ is set to $\rho = 0.25$ for both communication ends. Channel Profile E (large indoor space) from [10] has been used to generate the channel realisations used in the simulations. The CSIT-independent precoder component uses rotated Walsh-Hadamard matrices to spread the information in the frequency domain. Results are presented for a transmission mode based on QPSK modulation and 1/2-coding rate (no puncturing). Results with other modes lead to similar conclusions.

Figure 3 shows frame error rate (FER) results for different detection strategies, all based on soft information. In particular, a comparison is made between a system with no spreading (i.e., $Q = 1, \mathbf{C} = \mathbf{I}_{N_s}$) and a

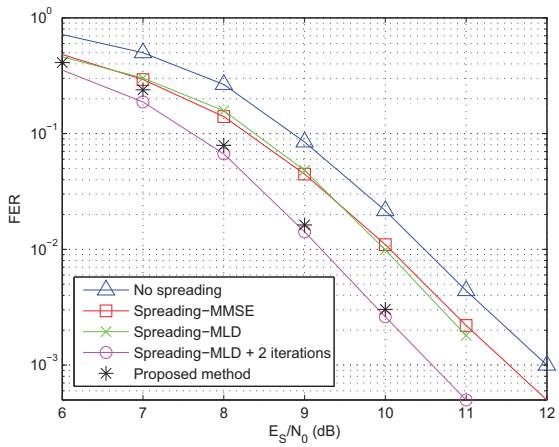

Figure 3: FER results for different detection strategies.

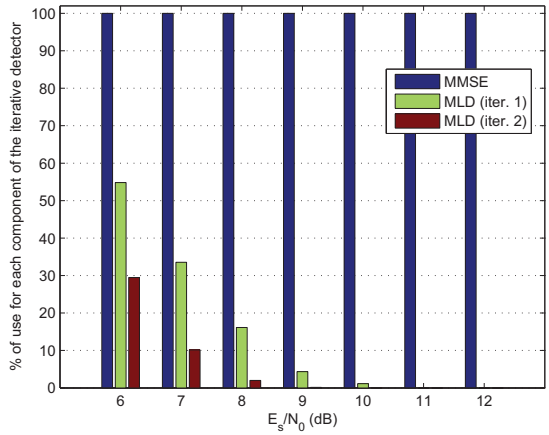

Figure 4: MMSE/MLD usage of the proposed detector.

system configured to spread the information among 4 subcarriers (i.e., $Q = 4, \mathbf{C} = \mathbf{I}_{Ns} \otimes \mathbf{C}_{fre}$). In the non-spread system case, all detection strategies (MMSE, MLD, iterative) perform identically [5] and this FER curve is included to serve as a reference baseline to which spread schemes can be compared to. When spreading takes place without using iterative detection, MLD and MMSE still perform rather similarly, although the MLD advantage tends to widen when increasing either constellation order (M) or the number of streams (N_s). As it can be observed in Fig. 3, the most significant advantage comes when iterative detection is applied in conjuction with MLD, where a gain 1-1.5 dB can be appreciated with respect to the rest of strategies over the usually relevant range of FER values ($10^{-1} - 10^{-3}$). As it has been previously mentioned, combining iterative detection with MMSE does not lead to any performace benefit. Nevertheless, in the case of iterative MLD, and given the much larger computational cost of evaluating (10) (MLD) instead of (9) (MMSE), the prize to pay is a large increase in computational complexity, which is the issue specifically targetted by the proposed hybrid iterative MMSE/MLD presented in the previous section and whose performance is shown to be nearly the same as the full blown iterative MLD receiver but with a much lower computational complexity thanks to the exploitation of the information provided by the CRC. To highlight this fact, Fig. 4 presents a histogram of the utilisation (in %) of the different components in the proposed iterative detector when generating the results in Fig. 3. Since the MMSE intervenes in the detection of all packets, its utilisation is 100% for all SNRs. In contrast, it can be clearly appreciated that the utilisation of the MLD components diminishes drastically with increasing SNR and, in fact, for most practical FER values (SNR ≥ 8 dB) the utilisation of MLD becomes marginal.

5. CONCLUSIONS

This paper has presented a hybrid linear/non-linear iterative detection strategy for linearly precoded MIMO-OFDM systems. The proposed technique has been shown to perform optimally from an error rate point of view while its complexity is only marginally superior to that of the simple linear MMSE (soft) detector. These properties make the proposed architecture most suitable for downlink scenarios where the receiver typically operates under tight power consumption constraints.

REFERENCES

[1] M. Costa, "Writing on dirty paper," *IEEE Trans. Information Theory*, vol. 29, no. 3, May 1983.

[2] D. Palomar, J. Cioffi, and M. Lagunas, "Joint tx-rx beamforming design for multicarrier MIMO channels: a unified framework for convex optimization," *IEEE Trans. Signal Processing*, vol. 51, no. 9, Sept. 2003.

[3] F. Riera-Palou, G. Femenias, and J. Ramis, "On the design of uplink and downlink group-orthogonal multicarrier wireless systems," *IEEE Trans. Communications*, vol. 56, no. 10, pp. 1656–1665, Oct. 2008.

[4] X. Yuan, C. Xu, L. Ping, and X. Lin, "Precoder design for multiuser MIMO ISI channels based on iterative LMMSE detection," *IEEE J. of Sel. Topics in Sig. Process.*, vol. 3, no. 6, pp. 1118 –1128, Dec. 2009.

[5] F. Riera-Palou and G. Femenias, "Space-frequency linear precoding with optimal detection for MIMO-OFDM systems," in *IFIP/IEEE Wireless Days*, Venice (Italy), Oct. 2010.

[6] B. Hassibi and H. Vikalo, "On the sphere-decoding algorithm I. Expected complexity," *IEEE Trans. Signal Processing*, vol. 53, pp. 2806–2818, Aug. 2005.

[7] F. Tosato and P. Bisaglia, "Simplified soft-output demapper for binary interleaved COFDM with application to HIPERLAN/2," in *Proc. IEEE ICC*, June 2002.

[8] E. Zimmermann and G. Fettweis, "Adaptive vs. hybrid iterative MIMO receivers based on MMSE linear and soft-SIC detection," in *IEEE PIMRC*, Sept. 2006.

[9] B. Hochwald and S. ten Brink, "Achieving near-capacity on a multiple-antenna channel," *IEEE Trans. Communications*, vol. 51, pp. 389–399, March 2003.

[10] V. Erceg, "Indoor MIMO WLAN Channel Models. doc.: IEEE 802.11-03/871r0," Draft proposal, Nov. 2003.